

Dynamic Characteristics of a Narrowband Land Mobile Communication Channel

H. Allen Barger, *Member, IEEE*

Abstract— Land mobile communication signals are subject to propagation effects that result in variation of received signal amplitude and phase. The most rapid signal variations are the result of multipath propagation and occur with sufficient severity to make reception difficult. At microwave frequencies, the narrowband (30-kHz) channel is considered nondispersive. It will experience flat amplitude fading and band-limited frequency distortion. An understanding of the dynamic nature of the communication channel is required to design land mobile systems that are tolerant of rapid multipath conditions. In this paper, a model is presented to characterize the dynamic nature of multipath channels, and a new dynamic measure, fractional power change rate, is introduced. Distribution of the fractional power change rate, power change rate, and phase change rate are predicted by the model and validated by comparison to measured data. The research in this paper is part of an ongoing effort to develop multipath-tolerant demodulation techniques for higher order modulation types. The measures developed herein are of primary importance for specifying the dynamic requirements for such demodulators.

Index Terms— Channel model, multipath, multipath propagation, narrowband channels, narrowband communication channel.

I. INTRODUCTION

IN A LAND mobile communication channel, movement of a communicating vehicle or of a nearby object will result in varying multipath propagation. In these multipath environments that involve a moving transmitter, receiver, or reflector, the receive signal amplitude and phase will change at rapid rates comparable to rates of change produced by the modulating signal. The rapid changes in amplitude and phase will be passed through the communication channel to the demodulator stage of the receiver. These changes are difficult to distinguish from the changes in amplitude and phase produced by modulation and are seen by the demodulator as noise. The phase and fractional power change rates may be used to characterize the multipath noise at the input of the receiver demodulator stage. The characterization of multipath noise provides the designer insight into the requirements for design of practical demodulators in order to tolerate or compensate for multipath. The variances of the phase change rate and the fractional power change rate may be used to represent multipath noise power for computation of expected demodulator performance in the multipath channel.

By definition, the received multipath signal is a combination of multiple rays, each ray being a delayed and attenuated copy

of the original signal. Rays arrive at the receiver at various times and are combined in an additive manner. The combined signal is perceived by the receiver as a single ray that varies in amplitude and phase as the actual ray components cancel or add. In narrowband land mobile channels at typical cellular frequencies, the channel characteristics may be determined by examining the effects on a single unmodulated carrier passed through the channel. The resulting signal effects are measured by a receiver as apparent amplitude and phase modulation of the carrier.

A scattering model of the channel was used to predict dynamic characteristics, namely, rate of power change, rate of phase change, and fractional power change rate. The statistical distribution of these fractional power change and phase change rates match the Rice phase-rate Distribution. The power change rate was found to have a distribution characterized by a symmetrical modified Bessel function. The model predictions were verified by comparison to actual channel measurements. A test was conducted in both suburban and urban environments to provide measurement data. For the test, a UHF transmitter generated an unmodulated carrier at a nominal power level. This signal was transmitted into an outdoor shadowing environment, and the resulting signal collected from a moving vehicle and stored on magnetic media. The results were processed to extract dynamic channel characteristics.

Finally, the predicted and measured signal characteristics were compared to determine validity of the model for predicting dynamic channel characteristics and the measured data evaluated for insight into developing new channel models.

II. BACKGROUND

Much of the original theory and models used to characterize communication channels is based on work by Rice [1]–[3]. The Rice model presents four signal elements: amplitude, rate of amplitude change, phase, and rate of phase change. Channel statistics are then derived for a signal with additive Gaussian noise. Young presented the signal amplitude in multipath channels as having Rayleigh distribution and measured channel data to provide verification [4]. Jakes noted that received signal amplitude change rate multipath environments will be Gaussian in nature (central limit theorem) and presented Rice's basic equations as applicable to multipath channels [5]. He also presented frequency spectra of the amplitude waveform, frequency spectra due to random FM, and related maximum practical bandwidth (coherence bandwidth) to signal delay characteristics.

Manuscript received June 6, 1995; revised August 14, 1996.

The author is with the Electrical Engineering Department, University of Texas, Tyler, TX 75799 USA.

Publisher Item Identifier S 0018-9545(98)00689-6.

Long-term channel characteristics were separated from the short-term (dynamic) characteristics by Lee [6]–[8]. The long-term characteristics are attributed to shadowing and diffraction, a slow phenomena. Short-term characteristics are from changes in multipath experienced by the moving vehicle. Multipath was expressed in terms of pulse delay spread by Cox and measurements provided for both suburban and urban multipath channels using a pulsed signal source. The measured characteristics were then related to correlation bandwidth and expected Doppler effects [9], [10].

Physical models are essential to providing an understanding of the mechanism causing multipath characteristics. Ossanna's model predicted multipath fade characteristics, waveforms, power spectra, and frequency power spectra produced by a set of interfering waves reflected from the planar surfaces of buildings and houses in the vicinity of a mobile station [11]. Clarke produced a model that characterized the interfering signals as a set of random azimuthal waves, each having a random phase and arbitrary azimuth [12]. This scattering model was used to predict time and frequency domain channel characteristics. The frequency change due to multipath was found to mostly be within bounds established by twice the Doppler frequency. Aulin later expanded the Clarke scattering model to include a vertical distribution of signal sources [13].

III. CHANNEL MODEL

The three-dimensional (3-D) scattering model presented by Aulin was used as the basis for predicting channel behavior. Multipath signals are received as a composite resultant of a number of rays each originating at a diffraction or reflection point near the receive antenna. Each ray source is identical to the original, but delayed in time and decreased in amplitude. The resulting receive signal is perceived to be the original with amplitude and phase shift.

A. Slow Losses

Free-space loss results from spreading of the receive signal with distance and is usually given in the form of the Friis equation using the following [14]: P_r and P_t are the received and transmitted power, respectively, G_r and G_t receiver and transmitter antenna power gains, λ signal wavelength, and d distance from source to receiver

$$P_r = G_r G_t P_t (\lambda/4\pi d)^2. \quad (1)$$

In terms of received and transmitted amplitudes A_r and A_t , loss is given by

$$A_r = \sqrt{G_r} \sqrt{G_t} A_t (\lambda/4\pi d). \quad (2)$$

Terrain loss results from shadowing of the signal path by objects, or knife-edge diffraction of the signal around objects. Terrain loss varies with the rate the vehicle enters and leaves the shadowing or diffraction environment, which for most environments is much slower than multipath fade.

B. Dispersion, Delay Spread, and Coherence Bandwidth

By nature, multipath is a dispersive phenomena, spreading the received signal in time. For dispersion due to short time delays, multipath will result in a shift of signal amplitude and phase. If the path delay differences between rays are on the order of the time required to transmit one or more symbols, then dispersion of the receive signal will produce intersymbol interference (ISI) in addition to phase and amplitude variances. Delay spreads on the order of 1–3.5 μs are typical in urban environments with maximum delays of 9–10 μs [9]. For suburban environments, delay spreads on the order of 2 μs with maximum excess delays on the order of 5–7 μs should be expected [10]. Correlation bandwidth is a measure resulting from delay spread and is defined as the frequency separation between two closely spaced signals that will result in an envelope correlation of 0.5 or 0.9 when the signals are subjected to a given delay spread [15], [16]. For this application, we will consider the narrowband communication channel with a signaling rate of 24 kHz. This rate was chosen to be less than the channel coherence bandwidths of 40–250 kHz reported in earlier works [16]. At these low signaling rates, little ISI is produced, and the channel will be considered to be nondispersive. The short-term multipath effects that occur within a symbol period are termed “rapid fade” and “rapid phase change” rather than “dispersion.”

C. Random FM and Doppler

Rapid variations in the received signal phase are perceived by a detector to be variations in frequency and termed random FM [17]. In land mobile applications at 800–900-MHz cellular frequencies the bandwidth of random FM is on the order of the maximum Doppler frequency, the effects on systems using frequency modulation are nominally sub audible for highway speeds. This random FM will greatly impair digital transmission using direct carrier modulation.

D. Scattering Model for Multipath Dynamic Characteristics

Consider a single ray that travels from a fixed source location to a moving observer as shown in Fig. 1. Let the ray consist of a unity gain carrier; one that is reflected or refracted. The resulting ray, from the observer's perspective, may be described as

$$R_i(t) = A_i \left(\frac{\lambda}{4\pi d_i} \right) \cos[\omega(t - d_i/c)] \quad (3)$$

where A_i = Ray amplitude at the reflection location, $\lambda = c/f$ is the wavelength, d_i is the distance traveled from the reflection source, and c is the speed of light.

Rewriting (3) with the distance $d_{\lambda i}$ in phase delay, where $d_{\lambda i} = 2\pi d_i/\lambda$

$$R_i(t) = A_i \left(\frac{1}{2d_{\lambda i}} \right) \cos(\omega t - d_{\lambda i}). \quad (4)$$

The arrival angle ϑ_i is usually assumed to be uniformly distributed between $-\pi \leq \vartheta_i < \pi$. The velocity is limited by

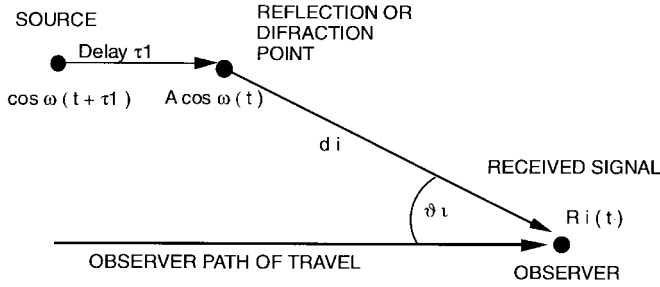


Fig. 1. Geometry of a single ray.

$-v \leq (d/dt)d_i \leq v$, and distance d_i varies as

$$\frac{d}{dt} d_i = v \cos \vartheta_i. \quad (5)$$

In a multipath environment, the signal seen by the observer is composed of multiple rays, each having the same form of $R_i(t)$. If received noise is ignored, the combined signal $R(t)$ as seen by the observer is given by

$$R(t) = \sum_i R_i(t) = \sum_i A_i (2d_{\lambda i})^{-1} \cos(\omega t - d_{\lambda i}). \quad (6)$$

An ideal receiver that produces complex baseband output will convert this signal into two components, in-phase (I) and quadrature (Q). These components may be represented by

$$\begin{aligned} I &= \text{LPF} \left\{ 2 \cos(\omega t) \sum_i A_i (2d_{\lambda i})^{-1} \cos(\omega t - d_{\lambda i}) \right\} \\ &= \text{LPF} \left\{ 2 \sum_i A_i (2d_{\lambda i})^{-1} \left[\frac{1}{2} \cos(\omega t + \omega t - d_{\lambda i}) \right. \right. \\ &\quad \left. \left. + \frac{1}{2} \cos(\omega t - \omega t + d_{\lambda i}) \right] \right\} \\ &= \sum_i A_i \frac{1}{2d_{\lambda i}} \cos(d_{\lambda i}) \end{aligned} \quad (7)$$

$$\begin{aligned} Q &= \text{LPF} \left\{ 2 \sin(\omega t) \sum_i A_i (2d_{\lambda i})^{-1} \cos(\omega t - d_{\lambda i}) \right\} \\ &= \sum_i A_i \frac{1}{2d_{\lambda i}} \sin(d_{\lambda i}) \end{aligned} \quad (8)$$

where $\text{LPF}\{a\}$ is the notation for "low-pass filtering." From the two components I and Q , the instantaneous amplitude (amp), power (pwr), and phase (ϕ) of the composite received signal are expressed as [18]

$$\begin{aligned} \text{pwr} &= I^2 + Q^2 \\ &= \left[\sum_i A_i \frac{1}{2d_{\lambda i}} \cos(d_{\lambda i}) \right]^2 \\ &\quad + \left[\sum_i A_i \frac{1}{2d_{\lambda i}} \sin(d_{\lambda i}) \right]^2 \\ \text{amp} &= \sqrt{I^2 + Q^2} \end{aligned} \quad (9)$$

$$= \sqrt{\left[\sum_i A_i \frac{1}{2d_{\lambda i}} \cos(d_{\lambda i}) \right]^2 + \left[\sum_i A_i \frac{1}{2d_{\lambda i}} \sin(d_{\lambda i}) \right]^2} \quad (10)$$

$$\begin{aligned} \phi &= \tan^{-1}(Q/I) \\ &= \tan^{-1} \frac{\sum_i A_i \frac{1}{2d_{\lambda i}} \sin(d_{\lambda i})}{\sum_i A_i \frac{1}{2d_{\lambda i}} \cos(d_{\lambda i})}. \end{aligned} \quad (11)$$

The change rates of power and phase of a received signal are given by their first derivatives. In addition, fractional power change rate is defined as the fraction of nominal power the signal may change in unit time and may be scaled in terms of decibel/s or percent/s. Dynamic parameters are presented in terms of I and Q in the following equations:

$$\begin{aligned} \text{pwr}' &= \frac{d}{dt} (\text{pwr}) = \frac{d}{dt} (I^2 + Q^2) \\ &= 2I dI/dt + 2Q dQ/dt \end{aligned} \quad (12)$$

$$\begin{aligned} \phi' &= \frac{d}{dt} (\phi) = \frac{d}{dt} [\tan^{-1}(Q/I)] \\ &= \frac{2I dQ/dt - 2Q dI/dt}{(I^2 + Q^2)} \end{aligned} \quad (13)$$

$$\begin{aligned} \frac{\text{pwr}'}{\text{pwr}} &= \frac{1}{\text{pwr}} \frac{d}{dt} (\text{pwr}) \\ &= \frac{2I dI/dt + 2Q dQ/dt}{(I^2 + Q^2)} \end{aligned} \quad (14)$$

$$\begin{aligned} \text{amp}' &= \frac{d}{dt} (\text{amp}) = \frac{d}{dt} \sqrt{I^2 + Q^2} \\ &= \frac{2I dI/dt + 2Q dQ/dt}{(I^2 + Q^2)^{3/2}}. \end{aligned} \quad (15)$$

E. Power Change Rate

The pdf's of each dynamic variable are needed. To derive the pdf of pwr' , expressions for I and Q from (7) and (8) are substituted into (12)

$$\begin{aligned} \text{pwr}' &= 2 \left[\sum_i A_i \frac{1}{2d_{\lambda i}} \cos(d_{\lambda i}) \right] \\ &\quad \cdot \left[-\sum_i A_i \frac{1}{2d_{\lambda i}^2} \cos(d_{\lambda i}) C_i \right. \\ &\quad \left. - \sum_i A_i \frac{1}{2d_{\lambda i}} \sin(d_{\lambda i}) C_i \right] \\ &\quad + 2 \left[\sum_i A_i \frac{1}{2d_{\lambda i}} \sin(d_{\lambda i}) \right] \\ &\quad \cdot \left[-\sum_i A_i \frac{1}{2d_{\lambda i}^2} \sin(d_{\lambda i}) C_i \right. \\ &\quad \left. + \sum_i A_i \frac{1}{2d_{\lambda i}} \cos(d_{\lambda i}) C_i \right] \end{aligned} \quad (16)$$

where $C_i = d/dt(d_{\lambda i})$ and is a random variable that may be considered to be independent of $d_{\lambda i}$. For most situations, the observer is on the order of 10–1000 wavelengths from most reflection sources, so $d_{\lambda i}^{-1} \gg d_{\lambda i}^{-2}$, and thus

$$\begin{aligned} \text{pwr}' \cong & \frac{1}{2} \left[\sum_i A_i d_{\lambda i}^{-1} \cos(d_{\lambda i}) \right] \\ & \cdot \left[-\sum_i C_i A_i d_{\lambda i}^{-1} \sin(d_{\lambda i}) \right] \\ & + \frac{1}{2} \left[\sum_i A_i d_{\lambda i}^{-1} \sin(d_{\lambda i}) \right] \\ & \cdot \left[\sum_i C_i A_i d_{\lambda i}^{-1} \cos(d_{\lambda i}) \right] \end{aligned} \quad (17)$$

pwr' is of the form $\frac{1}{2}(XY + VW)$, where

$$\begin{cases} X = \sum_i A_i d_{\lambda i}^{-1} \cos(d_{\lambda i}) \\ Y = -\sum_i C_i A_i d_{\lambda i}^{-1} \sin(d_{\lambda i}) \\ V = \sum_i A_i d_{\lambda i}^{-1} \sin(d_{\lambda i}) \\ W = \sum_i C_i A_i d_{\lambda i}^{-1} \cos(d_{\lambda i}) \end{cases} \quad (18)$$

V , W , X , and Y are each composed of the sum of a group of random numbers and thus may be treated as zero mean Gaussian random variables (central limit theorem). Furthermore, V and W are independent of each other and, likewise, X and Y . However, the products XY and VW are not independent. The pdf's of V and W are of the same form of that for X and Y , having variances σ_x^2 and σ_y^2

$$\left\{ \text{pdf}(x) = \frac{e^{-(x^2/2\sigma_x^2)}}{\sqrt{2\pi}\sigma_x}, \quad \text{pdf}(y) = \frac{e^{-(y^2/2\sigma_y^2)}}{\sqrt{2\pi}\sigma_y} \right\}. \quad (19)$$

Equation (17) may be expanded as follows:

$$\begin{aligned} \text{pwr}' &= \frac{1}{2} \left\{ \sum_{i \neq j} A_i d_{\lambda i}^{-1} \cos(d_{\lambda i}) \left[-\sum_j C_j A_j d_{\lambda j}^{-1} \sin(d_{\lambda j}) \right] \right\} \\ &+ \frac{1}{2} \left\{ \sum_{i \neq j} A_i d_{\lambda i}^{-1} \sin(d_{\lambda i}) \left[\sum_j C_j A_j d_{\lambda j}^{-1} \cos(d_{\lambda j}) \right] \right\} \\ &- \frac{1}{2} \left[\sum_i A_i d_{\lambda i}^{-1} \cos(d_{\lambda i}) C_i A_i d_{\lambda i}^{-1} \sin(d_{\lambda i}) \right] \\ &+ \frac{1}{2} \left[\sum_i A_i d_{\lambda i}^{-1} \sin(d_{\lambda i}) C_i A_i d_{\lambda i}^{-1} \cos(d_{\lambda i}) \right]. \end{aligned} \quad (20)$$

Note that the last two terms are identical and opposite in sign, thus

$$\begin{aligned} \text{pwr}' = & \frac{1}{2} \left\{ \sum_{i \neq j} A_i d_{\lambda i}^{-1} \cos(d_{\lambda i}) \right. \\ & \cdot \left[-\sum_j C_j A_j d_{\lambda j}^{-1} \sin(d_{\lambda j}) \right] \left. \right\} \\ & + \frac{1}{2} \left\{ \sum_{i \neq j} A_i d_{\lambda i}^{-1} \sin(d_{\lambda i}) \right. \\ & \cdot \left[-\sum_j C_j A_j d_{\lambda j}^{-1} \cos(d_{\lambda j}) \right] \left. \right\}. \end{aligned} \quad (21)$$

The term C_i may be seen as a randomizing vector applied to each term. The two terms have the same distribution and without the randomizing vector would be identical and opposite in sign. Measured data indicates that the joint probability of the combined terms is of the same form of either term taken singularly, thus the distribution of pwr' may be written as

$$\begin{aligned} \text{pwr}' \text{ '}' = & \frac{1}{2} \left\{ \sum_{i \neq j} A_i d_{\lambda i}^{-1} \cos(d_{\lambda i}) \right. \\ & \cdot \left[\sum_j C_j A_j d_{\lambda j}^{-1} \sin(d_{\lambda j}) \right] \left. \right\} \\ \text{'}' = & \frac{1}{2} XY \end{aligned} \quad (22)$$

where '=' is a notation to indicate having the same distribution.

Solving for the pdf of pwr' , let $Z = XY$, then $y = z/x$, and

$$\begin{aligned} \text{pdf}(z) &= \int_{-\infty}^{\infty} \frac{1}{x} f_{XY}(x, z/x) dx \\ &= \int_{-\infty}^{\infty} \frac{1}{x} \frac{e^{-(x^2/2\sigma_x^2)}}{\sqrt{2\pi}\sigma_x} \frac{e^{-(z/x)^2/2\sigma_y^2}}{\sqrt{2\pi}\sigma_y} dx \\ &= \frac{1}{2\pi\sigma_x\sigma_y} \int_{-\infty}^{\infty} \frac{1}{x} e^{-(x^2/2\sigma_x^2)} e^{-(z/x)^2/2\sigma_y^2} dx \end{aligned} \quad (23)$$

and letting $\sigma_x = \sigma_y = \sigma$ [19]

$$\begin{aligned} \text{pdf}(z) &= \frac{1}{2\pi\sigma^2} \int_{-\infty}^{\infty} x^{-1} e^{-[x^2/2\sigma^2 + (z^2/2\sigma^2)/x^2]} dx \\ &= K_o(2\sqrt{(1/2\sigma^2)(z^2/2\sigma^2)}) = K_o(|z|/\sigma^2) \\ &= \text{pdf}(\text{pwr}') \end{aligned} \quad (24)$$

where K_o represents the modified Bessel Function [20].

The signal level change rate may also be determined using signal amplitude rather than power. Amplitude change rate was shown to be Gaussian and is given by the following equation, where r is signal amplitude and the change rate has variance σ^2 [21]:

$$\text{pdf}(\text{amp}') = \frac{1}{\sqrt{4\pi}\sigma^2} e^{-r'^2/2\sigma^2}. \quad (25)$$

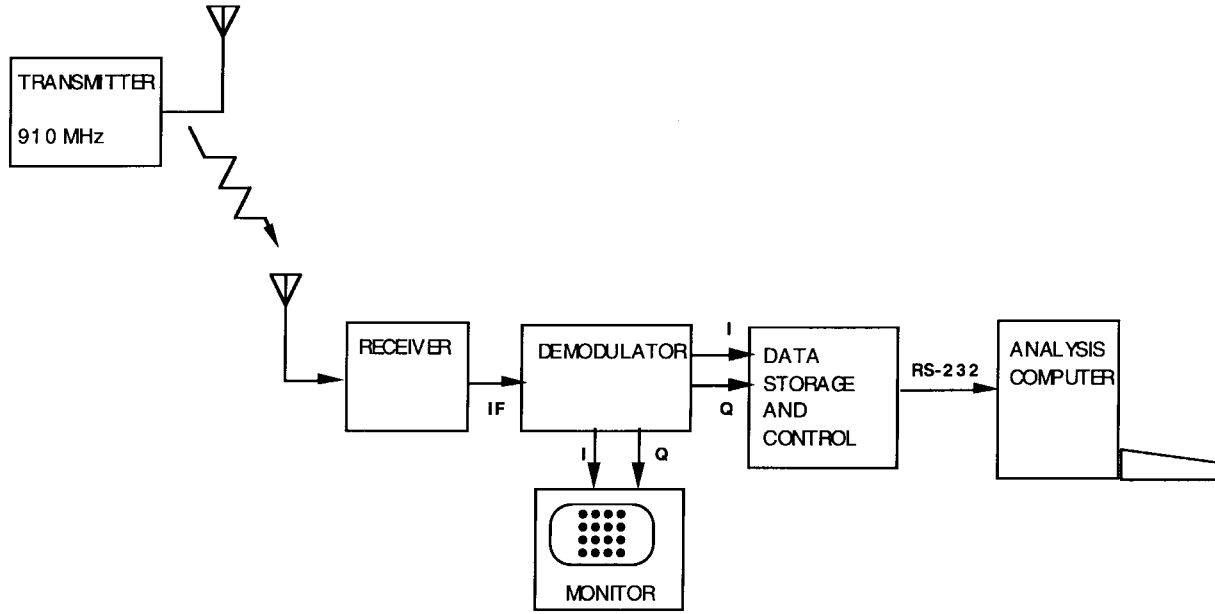


Fig. 2. Equipment used to measure multipath characteristics.

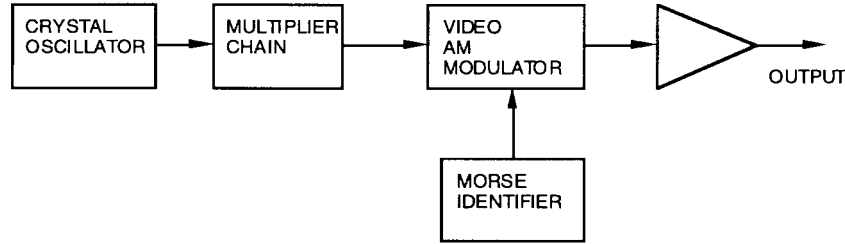


Fig. 3. Block diagram of the transmitter.

F. Phase Change Rate

The pdf of ϕ' may be expressed using (13) as

$$\begin{aligned} \text{pdf}(\phi') &= \text{pdf}\left\{\frac{d}{dt}[\tan^{-1}(Q/I)]\right\} \\ &= \text{pdf}\left[\frac{I dQ/dt - Q dI/dt}{(I^2 + Q^2)}\right]. \end{aligned} \quad (26)$$

I , Q , dI/dt , and dQ/dt are Gaussian distributed with zero mean. I and Q have the same variance σ_I^2 ; dI/dt and dQ/dt have variance σ_2^2 . The pdf of ϕ' is given by Jakes to be the Rice phase-rate distribution shown below [22]

$$\text{pdf}(\phi') = \frac{1}{2} \sqrt{\frac{b_0}{b_2}} \left[1 + \frac{b_0}{b_2} (\phi')^2\right]^{-3/2} \quad (27)$$

where b_0 and b_2 are the variances of amplitude and amplitude change rate, respectively.

G. Fractional Power Change Rate

Letting $s =$ the fractional power change rate pwr'/pwr , the pdf may be expressed using (16) to be identical with that for

(26). Letting s represent (pwr'/pwr)

$$\begin{aligned} \text{pdf}(s) &= \text{pdf}\left[\frac{I dI/dt + Q dQ/dt}{(I^2 + Q^2)}\right] \\ &= \text{pdf}\left[\frac{I dQ/dt - Q dI/dt}{(I^2 + Q^2)}\right] \\ &= \frac{1}{2} \frac{\sigma_a}{\sigma_b} \frac{1}{(1 + \phi'^2 \sigma_a^2 / \sigma_b^2)^{3/2}} \end{aligned} \quad (28)$$

where the variances σ_a^2 and σ_b^2 are the same as b_0 and b_2 in (27). Another derivation of the pdf of this combination of four Gaussian random variables is given in Appendix A.

IV. MEASUREMENTS

The measurement equipment consisted of a transmitter, antennas, receiver/data-acquisition system (DAS), mobile platform, and analysis workstation assembled as shown in Fig. 2.

The UHF transmitter provides a 910.25-MHz carrier at a nominal power of 0.2 W. A block diagram of the transmitter is shown in Fig. 3. A television exciter was used for the transmitter. It was frequency stabilized by use of thermal

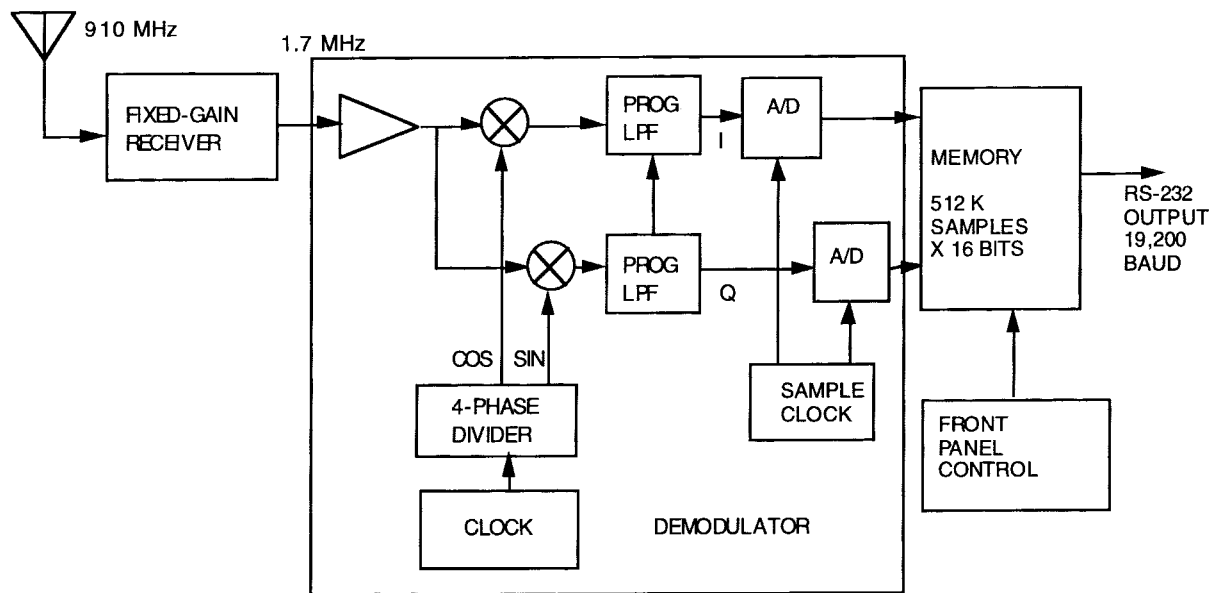


Fig. 4. Block diagram of the DAS.

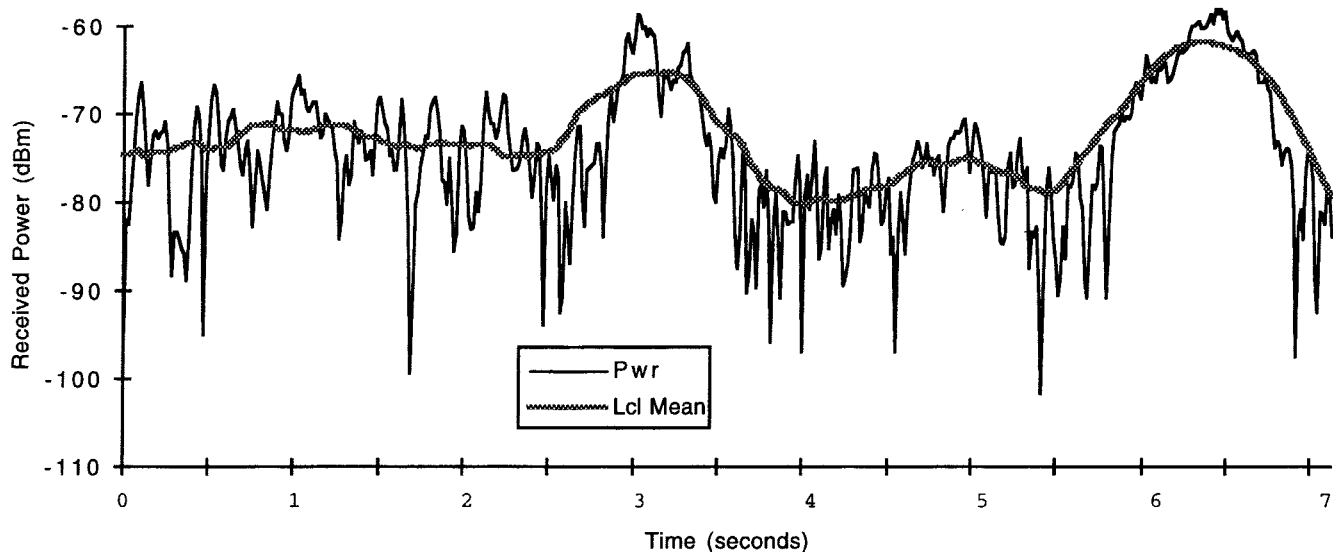


Fig. 5. Received power and local mean received power over a 7-s period for a suburban area multipath collection taken at 22 ft/s.

insulation and a regulated power supply. In the suburban environment, the transmit antenna was positioned 2 m above ground level to produce a low angle of radiation similar to that of a typical cellular transmitter antenna at a distance of about 1 km. Urban measurements were made using the transmit antenna mounted at approximately 70-ft elevation.

The mobile DAS consisted of a vehicle mounted antenna 2 m above street level, a simple microwave receiver having fixed gain and a complex (I/Q) demodulator, and a digital data recording system to collect demodulator output. Tests were made at a vehicle speed of 15 mph so results may be compared to available literature containing multipath amplitude fade data [23], [24]. The DAS is constructed as shown in Fig. 4. A triple-conversion fixed gain receiver provided 1.7-MHz IF to a complex demodulator. The signal is separated into I and Q components by the demodulator, and the output is filtered

to remove the fundamental and harmonic components of the beat frequency oscillator. Both the I and Q channels are synchronously digitized with separate 10-b analog-to-digital (A/D) converters sampling at 35 156.25 Hz. The digitized output is then stored in on-board memory for later transfer to the analysis computer. On-board memory contains 1 Mb of storage for 262 144 samples of complex waveform.

A Macintosh LC-III computer was used for data analysis. The analysis program was constructed to allow inspection of collected data in either numerical or graphical form. Data files were preprocessed to filter noise and provide accurate dc bias restoration. Data from both I and Q channels is low-pass filtered with 42-tap digital Kaiser filters [25]. The filter also averages samples of the signal using a weighted window. This averaging of the signal added about 2 b of resolution to the digitized values using noise for dithering.

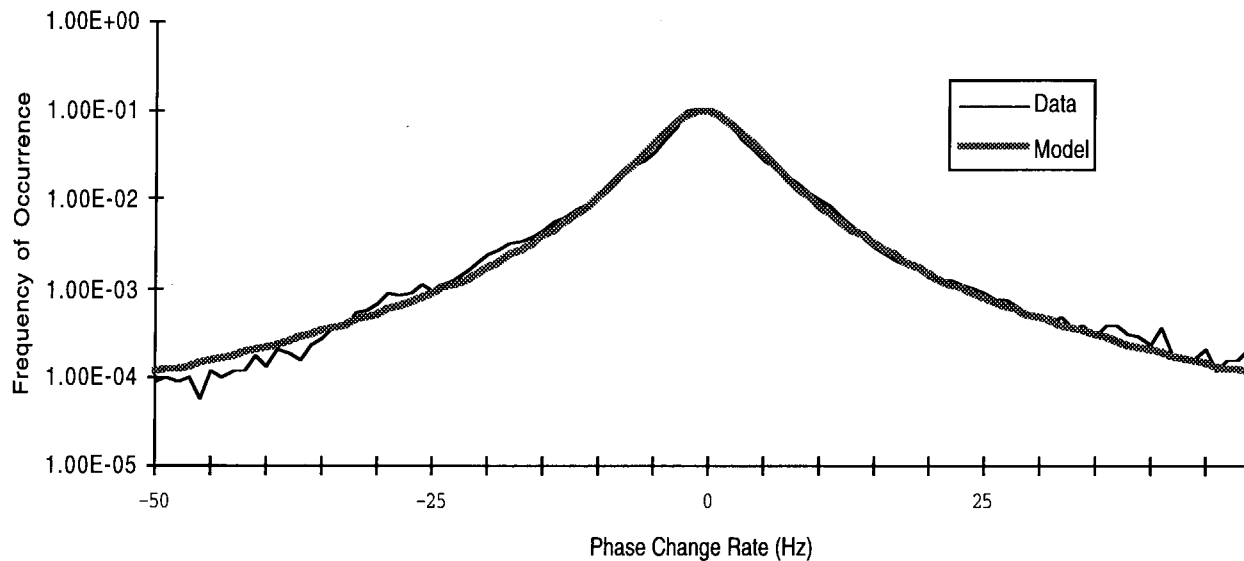


Fig. 6. Histogram of delta phase rate from the local mean value, suburban multipath.

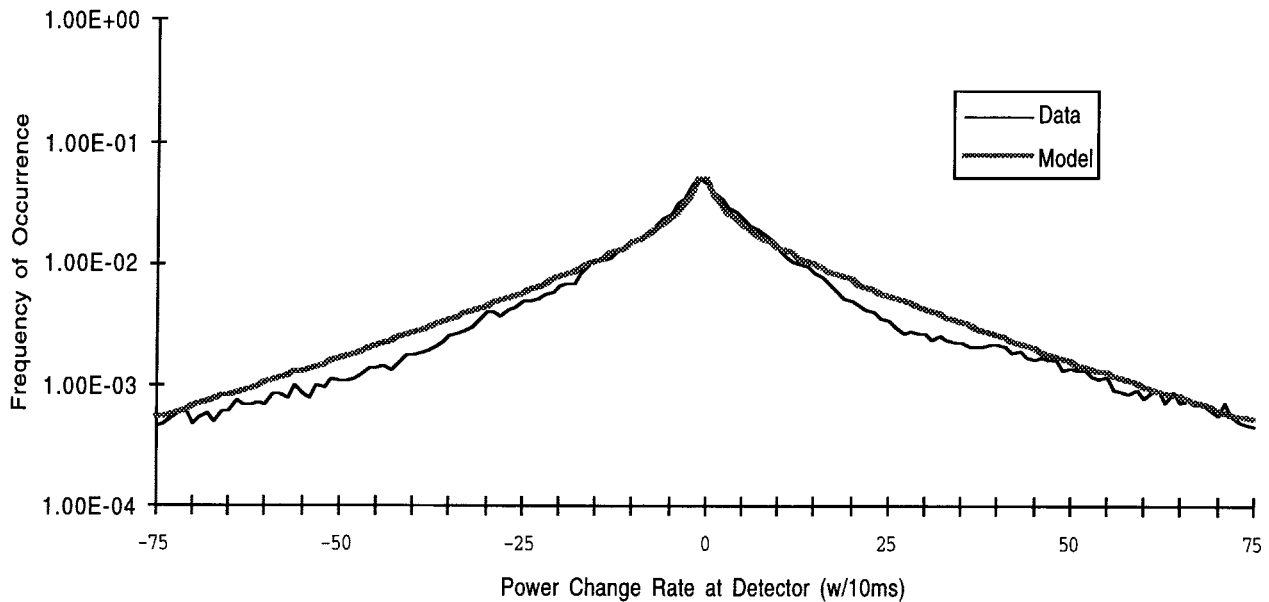


Fig. 7. Histogram of power change rate, suburban multipath.

A. Experimental Results

Received power of a typical suburban test run is shown in Fig. 5. The local mean of the signal, averaged over a sliding window of 1 s is shown superimposed on the graph. During this measurement the transmitter was not in direct line-of-sight from the test vehicle. Movement was in a straight line with the transmitter directly to the left side of the vehicle. Note peaks in the signal at about 2.9 and 6.4 s. These peaks correspond to the gaps between houses in the suburban development separated by approximately 80 ft.

The pdf of pwr' , pwr'/pwr , and ϕ' were created by histogramming the parameters over the entire collection period. Histograms of the rates of power and phase change for a suburban multipath measurement are shown in Figs. 6 and 7.

The experimental data is shown plotted with results predicted by the model.

The histogram for fractional power change rate is shown in Fig. 8, plotted with data predicted by the model.

V. CONCLUSION

A multiple-ray model was able to provide reasonable prediction of the probability distribution of the dynamic parameters of the land mobile multipath channel. The rate of phase change and fractional power change rate are both found to be distributed according to the Rice phase-rate distribution. The power change rate is distributed as a symmetrical modified Bessel function distribution.

The multipath dynamic rates are very rapid compared to the time constants normally chosen for receiver automatic-gain

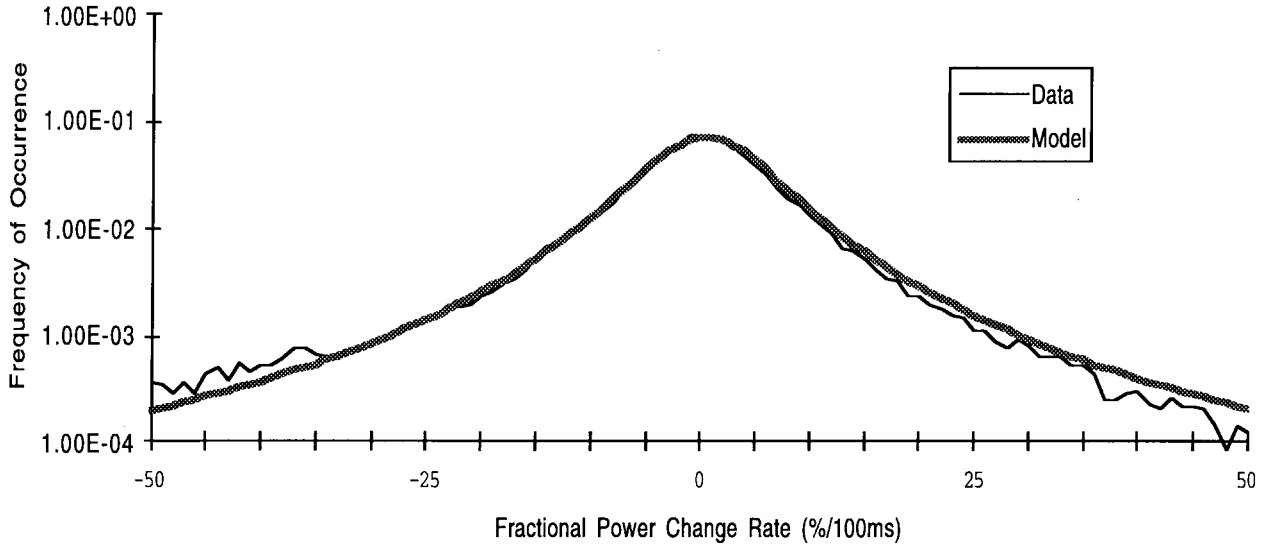


Fig. 8. Histogram of fractional power change rate, suburban multipath.

control (AGC), roughly 0.25–1.0 s, thus, the effects cannot be removed by AGC, but are passed to the demodulator. The dynamic parameters define multipath characteristics as seen by the detector stage of a receive system and thus are useful for defining requirements of a demodulator to process multipath. Demodulators designed to operate under these conditions should be able to process carriers that are directly modulated with high-rate digital information.

APPENDIX A

DISTRIBUTION OF FRACTIONAL POWER CHANGE RATE

Consider the random variable z composed of four elements given as

$$z = \frac{z_a z_c + z_b z_d}{z_a^2 + z_b^2}. \quad (29)$$

All terms z_a , z_b , z_c , and z_d are independent, and Gaussian-distributed zero-mean random variables z_a and z_c along with z_b and z_d have the same variance. The joint distribution of the terms may be written as

$$p(z_a, z_b, z_c, z_d) = \frac{e^{-(z_a^2 + z_b^2 + z_c^2 + z_d^2)/2}}{(2\pi)^2}. \quad (30)$$

The distribution of the numerator and denominator terms in (29) are obtained by transforming the z variables into the form given by u_a to u_d , where the transformation is represented by

$$\{u_a = z_a, u_b = \sqrt{z_a^2 + z_b^2}, u_c = z_c, u_d = z_a z_c + z_b z_d\} \quad (31)$$

and the inverse transformation represented by

$$\left\{ z_a = u_a, z_b = \sqrt{u_b^2 - u_a^2}, z_c = u_c, z_d = \frac{u_d - u_a u_c}{\sqrt{u_b^2 - u_a^2}} \right\}. \quad (32)$$

After algebraic manipulation, we obtain

$$\begin{aligned} p(u_a, u_b, u_d) &= \frac{u_b \exp \left\{ - \left[\frac{u_b^4 - u_a^2 u_b^2 + u_d^2 - u_a^2 u_d^2}{u_b^2 - u_a^2} \right] / 2 \right\}}{2\pi^2 (u_b^2 - u_a^2)} \\ &\cdot \int_{-\infty}^{\infty} \exp \left\{ - \left[\frac{\left(u_c - \frac{u_a u_d}{u_b^2} \right)^2}{2 \frac{u_b^2 - u_a^2}{u_b^2}} \right] \right\} du_c. \end{aligned} \quad (33)$$

Note the integral is of a normal distribution with mean $u_a u_d / u_b^2$ and variance of $(u_b^2 - u_a^2) / u_b^2$. This reduces to

$$\begin{aligned} p(u_a, u_b, u_d) &= \frac{u_b \exp \left\{ - \left[\frac{u_b^4 - u_a^2 u_b^2 + u_d^2 - (u_a^2 u_d^2) / u_b^2}{u_b^2 - u_a^2} \right] / 2 \right\}}{\sqrt{2\pi} \frac{2\pi^2 (u_b^2 - u_a^2)}{u_b^2}} \\ &\cdot \sqrt{\frac{u_b^2 - u_a^2}{u_b^2}} \end{aligned} \quad (34)$$

so simplifying with algebra

$$p(u_a, u_b, u_d) = \frac{1}{\sqrt{2\pi}^{3/2} \sqrt{u_b^2 - u_a^2}} e^{-[(u_b^2 + u_d^2 / u_b^2)] / 2} \quad (35)$$

integrating to remove u_a

$$\begin{aligned} p(u_b, u_d) &= \frac{1}{\sqrt{2\pi}^{3/2}} e^{-[(u_b^2 + u_d^2 / u_b^2)] / 2} \\ &\cdot \int_{-u_b}^{u_b} \frac{1}{\sqrt{u_b^2 - u_a^2}} du_a \\ &= \frac{1}{\sqrt{2\pi}} e^{-[u_b^4 + u_d^2 / u_b^2] / 2} \end{aligned} \quad (36)$$

making a final change of variables,

$$\{v = u_b, u_b = v, w = u_d / u_b^2, u_d = w v^2\} \quad (37)$$

and noting that

$$w = \frac{u_d}{u_b^2} = \frac{z_a z_c + z_b z_d}{(\sqrt{z_a^2 + z_b^2})^2} = \frac{z_a z_c + z_b z_d}{z_a^2 + z_b^2}. \quad (38)$$

Then

$$\begin{aligned} p(v, w) &= \frac{v^2}{\sqrt{2\pi}} e^{-(v^4 + w^2 v^4 / v^2) / 2} \\ &= \frac{v^2}{\sqrt{2\pi}} e^{-v^2(1+w^2)/2} \end{aligned} \quad (39)$$

integrating over v to solve for the probability of w , so

$$p(w) = \int_{-\infty}^{\infty} \frac{v^2}{\sqrt{2\pi}} e^{-v^2(1+w^2)/2} dv = \frac{1}{2(1+w^2)^{3/2}}. \quad (40)$$

Now, letting z_a and z_b have the same variance as do z_c and z_d and making the following substitutions and transforming z into s as follows:

$$\left\{ z_a = \frac{x_a}{\sigma_a}, z_b = \frac{x_b}{\sigma_a}, z_c = \frac{x_c}{\sigma_b}, z_d = \frac{x_d}{\sigma_b} \right\} \quad (41)$$

then s is represented as

$$\begin{aligned} s &= \frac{z_a z_c + z_b z_d}{z_a^2 + z_b^2} = \frac{x_a x_c / \sigma_1 \sigma_2 + x_b x_d / \sigma_a \sigma_b}{x_a^2 / \sigma_a^2 + x_b^2 / \sigma_b^2} \\ &= \frac{x_a x_c + x_b x_d}{x_a^2 + x_b^2} \frac{\sigma_a}{\sigma_2} = \frac{\sigma_a}{\sigma_b} w \end{aligned} \quad (42)$$

and the Jacobian

$$\mathbf{J} = \frac{ds}{dw} = \frac{\sigma_a}{\sigma_b} \quad (43)$$

so

$$p(s) = \frac{1}{2} |J| \frac{1}{(1+w^2)^{3/2}} = \frac{1}{2} \frac{\sigma_a}{\sigma_b} \frac{1}{(1+s^2 \sigma_b^2 / \sigma_a^2)^{3/2}}. \quad (44)$$

This solution was provided by A. D. Brock, Department of Mathematics, East Texas State University, Commerce, TX.

ACKNOWLEDGMENT

The author wishes to express gratitude to V. K. Prabhu for his support and guidance in the research project and help in preparation of this paper.

REFERENCES

- [1] S. O. Rice, "Mathematical analysis of random noise," *Bell Syst. Tech. J.*, vol. 23, pp. 282–332, July 1944.
- [2] ———, "Mathematical analysis of random noise," *Bell Syst. Tech. J.*, vol. 24, pp. 46–156, Jan. 1945.
- [3] ———, "Statistical properties of a sine wave plus random noise," *Bell Syst. Tech. J.*, vol. 27, no. 1, pp. 109–157, Jan. 1948.
- [4] W. R. Young, "Comparison of mobile radio transmission at 150, 450, 900, and 3700 Mc," in *Land-Mobile Communications Engineering*, D. Bodson, G. F. McClure, and S. R. McConoughey Eds. New York: IEEE Press, 1984, pp. 135–143.

- [5] W. C. Jakes, *Microwave Mobile Communications*. New York: IEEE Press, 1993.
- [6] W. C. Y. Lee, "Estimate of local average power of a mobile radio signal," *IEEE Trans. Veh. Technol.*, vol. VT-34, no. 1, pp. 22–27, 1985.
- [7] W. C. Y. Lee and Y. S. Yeh, "On the estimation of the second-order statistics of log-normal fading in mobile radio environment," *IEEE Trans. Commun.*, vol. COM-22, pp. 869–873, June 1974.
- [8] W. C. Y. Lee, *Mobile Communications Engineering*. New York: McGraw-Hill, 1982.
- [9] D. C. Cox and R. P. Leck, "Distribution of multipath delay spread and average excess delay for 910 MHz urban mobile radio path," *IEEE Trans. Antennas Propagat.*, vol. 23, pp. 206–213, Mar. 1975.
- [10] D. O. Cox, "Delay-Doppler characteristics of multipath propagation at 910 MHz in a suburban mobile radio environment," *IEEE Trans. Antennas Propagat.*, vol. 20, pp. 625–635, Sept. 1972.
- [11] J. F. Ossanna, Jr., "A model for mobile radio fading due to building reflections: Theoretical and experimental fading waveform power spectra," *Bell Syst. Tech. J.*, vol. 43, no. 6, pp. 2935–2971, Nov. 1964.
- [12] R. H. Clarke, "A statistical theory of mobile-radio reception," *Bell Syst. Tech. J.*, vol. 47, pp. 957–1000, July/Aug. 1968.
- [13] T. Aulin, "A modified model for the fading signal at a mobile radio channel," *IEEE Trans. Veh. Technol.*, vol. VT-28, no. 3, pp. 182–203, 1979.
- [14] H. T. Friis, "A note on a simple transmission formula," in *Proc. IRE*, 1946, p. 34.
- [15] W. C. Jakes, *Microwave Mobile Communications*. New York: IEEE Press, 1993, p. 51.
- [16] G. A. Arrendondo, J. C. Feggeler, and J. I. Smith, "Voice and data transmission," *Bell Syst. Tech. J.*, vol. 58, no. 1, pp. 97–122, Jan. 1979.
- [17] W. C. Jakes, *Microwave Mobile Communications*. New York: IEEE Press, 1993, pp. 39–45.
- [18] A. B. Carlson, *Communications Systems, An Introduction to Signals and Noise in Electrical Communication*. New York: McGraw-Hill, 1986.
- [19] I. S. Gradshteyn and I. M. Ryzhik, *Table of Integrals, Series, and Products*, 5th ed. San Diego, CA: Academic, 1994.
- [20] M. Abramowitz and I. A. Stegun, Eds., *Handbook of Mathematical Functions with Formulas, Graphs, and Mathematical Tables*. New York: Dover, 1964, p. 374.
- [21] W. C. Jakes, *Microwave Mobile Communications*. New York: IEEE Press, 1993, p. 34.
- [22] ———, *Microwave Mobile Communications*. New York: IEEE Press, 1993, p. 40.
- [23] ———, *Microwave Mobile Communications*. New York: IEEE Press, 1993, p. 14.
- [24] W. C. Y. Lee, *Mobile Communications Engineering*. New York: McGraw-Hill, 1982, p. 10.
- [25] A. V. Oppenheim and R. W. Schaffer, *Discrete Time Signal Processing*. Englewood Cliffs, NJ: Prentice-Hall, 1989, p. 455.



H. Allen Barger (M'90) received the B.S., M.S., and Ph.D. degrees in electrical engineering from the University of Texas at Arlington in 1975, 1979, and 1996, respectively.

From 1978 to 1982, he worked at the Collins Communication Systems Division of Rockwell International designing digital communication sub-systems. From 1982 to 1996, he worked at the Airborne Systems Division of Raytheon E-Systems as a Systems Engineer responsible for multiple projects in communications and computer applications. He is currently a Faculty Member in the Electrical Engineering Department, University of Texas at Tyler. His current interests are digital implementation of communication equipment, modulation techniques, and software architectures.